

## Synthesis of Cassava Starch-Grafted Polyacrylamide Hydrogel by Microwave-Assisted Method for Polymer Flooding

Maudy Pratiwi Novia Matovanni, Sperisa Distantina\*, and Mujtahid Kaavessina

Department of Chemical Engineering, Faculty of Engineering, Universitas Sebelas Maret,  
Jl. Ir. Sutami 36A, Kentingan, Surakarta 57126, Indonesia

\* **Corresponding author:**

email: sperisa\_distantina@staff.uns.ac.id

Received: December 18, 2021

Accepted: April 5, 2022

DOI: 10.22146/ijc.71343

**Abstract:** Cassava starch-grafted polyacrylamide (CS-g-PAM) hydrogels were synthesized using a microwave-assisted method and  $K_2O_8S_2$  (KPS) as an initiator. In this study, we studied the influence of the amount of acrylamide and irradiation time on the properties of CS-g-PAM. The characterization of CS-g-PAM obtained was shown by Fourier-transform infrared (FTIR) and Scanning Electron Microscope (SEM) analysis. To predict the behavior of the samples under reservoir conditions, the properties of CS-g-PAM, such as swelling ratio, water-solubility, and viscosity were determined as a function of temperature, salt concentration, and aging time. The FTIR spectra and SEM analysis of the CS-g-PAM confirmed that the polyacrylamide chains were successfully grafted onto the cassava starch backbone. The results showed that the increasing amount of acrylamide and the longer irradiation time improved the properties of CS-g-PAM. Preparation of CS-g-PAM with 10 g of acrylamide and 180 s of irradiation time resulted in the highest grafting percentage and water solubility, which was 1565.53 and 96.06%, respectively. Its viscosity also exceeded 97% after 15 days of aging. The results showed that CS-g-PAM expressed properties such as good thickening, temperature resistance, and salt resistance according to reservoir conditions. This finding indicated that CS-g-PAM has good potential for oil recovery applications.

**Keywords:** hydrogel; cassava starch; polyacrylamide; microwave-assisted; enhanced oil recovery

### ■ INTRODUCTION

Enhanced oil recovery (EOR) technology is urgently needed in the midst of a worsening energy crisis, such as declining oil production, high crude prices and ineffective primary production methods [1]. In the field of oil production, several methods are used to increase the recovery of the amount of oil and gas from the field. The most frequently injected fluid into oil wells is water, but water flooding still leaves around 60–70% of the oil contained in the reservoir [2]. Polymer flooding in the EOR system has evolved into a very efficient and cost-effective method. Polymer flooding is a process that has been used effectively in various oil fields across the world. Field investigations have indicated that polymer flooding can improve crude oil recovery by 5–30% from the original oil in place (OOIP) and by 3% following water

flooding. The efficiency of polymer flooding ranges from 0.7 to 1.75 lb of polymer per bbl of remaining oil output [3–4]. Even at extremely low concentrations, the polymer solution is injected with water to improve its viscosity and affect the mobility of the oil and reduce the permeability of the core [5]. Hydrogel is a polymer that can be used as polymer injection in EOR technology. However, hydrogel in high temperature and high salinity environments is usually affected by syneresis problems, which cause water to escape from the hydrogel phase [6]. Consequently, improving hydrogel stability is key to enhancing hydrogel performance for polymer flooding applications in difficult reservoir conditions.

The hydrogel can be made from natural or synthetic polymers or both. Graft copolymerization of natural polymers with functional synthetic polymers

results in modified products that combine the desired features of both the natural and the synthetic polymer in a single molecule [7]. The synthetic polymer commonly used for EOR applications is partially hydrolyzed polyacrylamide (HPAM). Synthetic polymers provide high flexibility in controlling the chemical structure of the polymer to increase the strength of the hydrogel and absorption capabilities [8]. However, the HPAM chain will collapse and disrupt the three-dimensional network structure of the polymer solution under high salinity and high temperature conditions [9]. Therefore, the viscosity of the HPAM solution will decrease drastically under difficult reservoir conditions (e.g., high temperature, high pressure, high salinity) leading to non-compliance with oilfield engineering application standards [10]. The use of synthetic polymers also has an adverse effect on the environment due to the toxicity and carcinogenicity of the residual monomers [11].

As a natural and renewable raw material with abundant supplies and no contamination, polysaccharides (xanthan, cellulose, and starch) can be used as raw materials for hydrogel synthesis and widely applied in polymer flooding procedures. Natural polymers have a greater resistance to salinity and temperature because of their unusual helical structure (triple or double), stiffness, and charge-free chains, which gives them excellent thickening and stability in adverse conditions reservoirs [11-12]. Natural polymers are cheap, readily available, biocompatible, biodegradable, and environmentally friendly [13]. Therefore, the synthesis of hydrogels from natural and synthetic materials can be an alternative to polymer synthesis that is environmentally friendly, inexpensive and has good resistance to reservoir conditions.

Several previous studies have reported hydrogel synthesis from a combination of natural and synthetic polymers for potential EOR. Previous studies have reported the synthesis of guar gum-based hydrogel by graft copolymerization using acrylamide and 2-acrylamido-2-methylpropane sulfonic acid (AMPS) and cross-linked using *N,N'*-methylene bisacrylamide (MBA) and potassium persulfate (KPS) as initiator. Guar gum-based hydrogel showed higher thermal stability than the

native guar gum [14]. Composite from rice straw waste, acrylamide (AM), vinyl methacrylate (VMA) was synthesized by free-radical emulsion polymerization using MBA as crosslinker and KPS as initiator. According to flooding experiments, the obtained composite has good resistance to thermal and ionic degradation [15]. Chitosan-modified polymer was synthesized by free radical polymerization with acrylic acid (AA) and acrylamide (AM). The solution properties of the polymer obtained showed better thickening ability and temperature and salt resistance than HPAM [16]. All syntheses mentioned above were done by polymerization using conventional thermal heating. Previous studies showed that natural and synthetic polymer modification successfully improved hydrogel stability.

According to several previous studies, grafting was performed by utilizing microwave energy, and the obtained hydrogel, CS-g-PAM hydrogel, may have the potential to be a candidate for EOR application. It has never been reported previously. The use of microwave increases the formation of copolymers, resulting in higher polymer products with a very short time required for polymer formation compared to conventional heating methods. To control the percentage of grafting, the microwave power and irradiation exposure time are controlled electronically [17].

In this study, we explore the influence of acrylamide amounts and irradiation time on the tolerance of reservoir properties of CS-g-PAM obtained as indicated by the swelling ratio of the hydrogel in water with various salt concentrations and temperatures, the viscosity of the polymer solution under reservoir conditions as a thickening agent, and the viscosity resistance of the polymer solution for 15 days. The successful grafting of polyacrylamide chains onto the backbone of cassava starch was characterized using Fourier-transform infrared (FTIR) and Scanning Electron Microscopy (SEM) analysis.

## ■ EXPERIMENTAL SECTION

### Materials

Cassava starch was obtained from a local market in Surakarta, Indonesia. Acrylamide (> 99%) and  $K_2O_8S_2$

(KPS) (> 99%) were purchased from E. Merck, Germany. Acetone (technical) was purchased from Saba Kimia, Surakarta, Indonesia. Sodium chloride (technical) was purchased from PT. Polimikro Berdikari Nusantara, Surakarta. All chemicals and reagents are used without additional treatment.

### Instrumentation

FTIR analysis was conducted on a Frontier FTIR spectrophotometer (Shimadzu, IRSpirit). The surface morphology was determined by JEOL Benchtop Scanning Electron Microscopy JCM 7000. Viscosity measurement was carried out on the Brookfield Viscometer DV2T.

### Procedure

#### Synthesis of cassava starch-grafted polyacrylamide

In this experiment, hydrogel polymer was synthesized by reacting cassava starch and acrylamide using KPS as the initiator and utilizing energy from domestic microwave radiation (Krisbow 20 L). CS-g-PAM was synthesized by varying the amount of acrylamide and the irradiation time, as shown in Table 1. One gram of cassava starch was added in 50 mL distilled water, then a certain amount of acrylamide and 0.3 g of KPS were added. The solution mixture of cassava starch, acrylamide, and KPS was put into a 1000 mL beaker and irradiated by microwave at 364 W. Microwave irradiation was carried out for 30 s until the solution approached the boiling temperature at < 70 °C, then the solution was cooled by immersing the beaker in cold water until the solution approached room temperature. Microwave irradiation – cooling cycle was repeated until a gel was formed and the irradiation time was determined (180 s or

6 cycles). There were 2 types of irradiation time. The first was stopped when the gel was formed and changed according to the amount of acrylamide. The second was the determined irradiation time (180 s), which was the same for all acrylamide amounts. The microwave irradiation – cooling cycle was carried out to minimize homopolymer formation reactions and to avoid vapors containing acrylamide monomers. After the microwave-assisted grafting process was completed, the gel material was allowed to stand for 24 h to complete the grafting reaction process. The gel material in the reaction vessel was soaked with excess acetone until a precipitate was formed. The CS-g-PAM precipitate was dried in an oven at 50 °C for 24 h. The percentage of grafting of CS-g-PAM obtained was calculated by the Eq. (1):

$$\% \text{grafting} = \frac{\text{mass of polyacrylamide grafted cassava starch} - \text{mass of cassava starch}}{\text{mass of cassava starch}} \times 100\% \quad (1)$$

The details of the synthesis of CS-g-PAM hydrogel are shown in Table 1.

#### Fourier transform infrared spectroscopy

FTIR spectra of cassava starch and CS-g-PAM (A–F) were analyzed on a Frontier FTIR spectrophotometer (Shimadzu, IRSpirit). CS-g-PAM obtained from various conditions was analyzed directly without forming pellets with KBr.

#### Scanning electron microscopy

The surface microstructure of cassava starch and CS-g-PAM (A–F) was determined by using JEOL Benchtop Scanning Electron Microscopy JCM 7000. The specimens were coated with gold and observed at 500–5000× magnification. The cassava starch had been gelatinized before SEM measurement.

**Table 1.** Various compositions for the synthesis of CS-g-PAM hydrogel

Code	Mass of cassava starch (g)	Mass of acrylamide (g)	Mass of KPS (g)	Irradiation time (s)	% Grafting
A	1	2	0.3	300	112.20
B	1	2	0.3	180	71.25
C	1	5	0.3	60	360.29
D	1	5	0.3	180	575.58
E	1	10	0.3	30	1237.32
F	1	10	0.3	180	1565.53

### Swelling test

The dried CS-g-PAM was weighed and recorded as  $W_1$  (g). The swelling test was determined by soaking  $W_1$  in 100 mL of distilled water with various swelling times, NaCl concentrations, and temperatures according to reservoir conditions. The swollen CS-g-PAM was measured as  $W_2$  (g). The swelling ratio was calculated using Eq. (2):

$$S = \frac{W_2 - W_1}{W_1} \quad (2)$$

### Water solubility measurement

One gram of CS-g-PAM was mixed in 100 mL of distilled water for 1 h, then filtered. The precipitated filter paper was dried in an atmospheric oven at 50 °C to a constant weight. The percentage of CS-g-PAM solubility in water was calculated by Eq. (3).

$$\text{Water solubility \% (w / w)} = \frac{W_0 - W_{\text{ins}}}{W_0} \quad (3)$$

where  $W_0$  is the initial weight of the CS-g-PAM (1 g), and  $W_{\text{ins}}$  is the weight of dried precipitated CS-g-PAM.

### Thickening ability

The dried CS-g-PAM was powdered and dissolved in distilled water at room temperature. The viscosity of polymer solutions with a concentration of 1 wt.% was measured in various NaCl concentrations and temperatures according to reservoir conditions. After preparing the polymer solution, viscosity measurement was carried out on the Brookfield Viscometer DV2T.

### Anti-aging ability

The viscosity of polymer solutions with a concentration of 1 wt.% was measured for 15 days in distilled water. Apparent viscosity was measured with a Brookfield Viscometer DV2T.

## ■ RESULTS AND DISCUSSION

### Synthesis of Cassava Starch-Polyacrylamide Hydrogel

The mechanism of the microwave-assisted grafting method consists of initiation, propagation, termination, and homopolymer formation (side reaction) [18]. The initiation phase occurs when a certain amount of initiator is added, and a microwave irradiates the reaction mixture.

The formation of complexes between the hydroxyl groups of polysaccharides and oxidants occurs due to the KPS mechanism that produces free radicals. Microwave radiation twists and stretches the bonds of acrylamide molecules. The electrons from the pi bond, where the C-C double bond will be extended, split into two locations (i.e., the free radical side of the constituent carbon atom). When free radical sites are formed in cassava starch (i.e., polymer backbone), monomers are added by chain propagation until the free radical sites are terminated via the termination step [19]. The termination step occurs when acetone is added to form a precipitate of the resulting CS-g-PAM. Here, microwave selectively excited polar bonds unlike heat energy and high energy radiation [18,20]. CS-g-PAM was synthesized through the interaction between free radical sites generated in the cassava starch backbone (by KPS) and free radical sites generated in acrylamide (by microwave radiation) through free radical reactions.

The microwave-assisted method with various initial conditions is shown in Table 1, where we can see that the irradiation time required for the gel to form decreased as the amount of acrylamide increased. The irradiation time required for the gel formation decreased from 300 to 30 s as the content of the acrylamide monomer increased from 2 to 10 g. Meanwhile, for the case of CS-g-PAM C, D, E, and F, when the irradiation time was extended to 180 s, the percentage of grafting obtained also increased. For the case of CS-g-PAM A and B, it had not yet formed a gel when the irradiation time was 180 s. Therefore, the irradiation time was extended, and the gel formation time was 300 s. The higher amount of acrylamide and the longer irradiation time increased the grafting percentage. The grafting percentage increased from 71.25 to 1565.53% as the amount of acrylamide increased from 2 to 10 g. The increase in grafting percentage and the decrease of irradiation time for the gel formation was due to the availability of excess monomer molecules to be grafted onto the polymer backbone at the propagation step.

In addition, because the proportion of cassava starch was smaller than acrylamide, the percentage of grafting was quite high. More homopolymerization

reactions occurred, and some of the homopolymers and grafted products were overlapped, entangled, or even twisted. Acetone extraction could not entirely remove these homopolymers [21].

### Fourier Transform Infrared Spectroscopy

The FTIR spectra of cassava starch (CS) and CS-g-PAM are shown in Fig. 1. The FTIR results of CS show the main absorption peaks, including:  $3304.71\text{ cm}^{-1}$  (OH strain vibration),  $2916.76\text{ cm}^{-1}$  (CH strain vibration), and C–O–C strain vibrations at  $1141.03\text{ cm}^{-1}$ ,  $1069.72\text{ cm}^{-1}$ , and  $1016.94\text{ cm}^{-1}$ .

All grafted products displayed identical profiles on the FTIR spectrum. Therefore, the discussion was carried out for CS-g-PAM A only as a representative for the entire grafted sample. In CS-g-PAM A, the O–H strain vibration of the starch hydroxyl group and the N–H strain vibration of the PAM amide group overlapped and led to a peak at  $3356.06\text{ cm}^{-1}$  and a shoulder peak at  $3197.74\text{ cm}^{-1}$ . A small peak at  $2929.60\text{ cm}^{-1}$  is associated with the C–H strain vibration. The peak at  $1019.80\text{ cm}^{-1}$  is assigned to the C–O–C strain vibration. The appearance of a sharp peak at  $1645.99\text{ cm}^{-1}$  is associated with C=O stretching while the peak at  $1596.02\text{ cm}^{-1}$  is associated with N–H. Furthermore,

another additional peak in the graft product at  $1336.43\text{ cm}^{-1}$ , indicates C–N stretching.

Fig. 1. shows that the peaks of O–H groups in CS-g-PAM is not as sharp compared to the CS. It was similar to FTIR spectra of starch-g-polyacrylamide [22] and cassava starch-polydiallyldimethylammonium chloride (polyDADMAC) [23]. It may be explained that the presence of O–H groups was replaced by polyacrylamide chains [22]. The presence of strain vibrations C=O, N–H, and C–N at  $-\text{CONH}_2$  also indicates the success of the grafting process. The FTIR spectra shown in Fig. 1. show that the graft copolymer is generated by the interaction between the free radical generated in the backbone of CS and polyacrylamide through the free radical reaction mechanism.

To support our data, the comparison of the FTIR spectra between CS-g-PAM A and other hydrogels from previous studies is shown in Table 2. In the FTIR spectra of the synthesis of cassava starch-graft-polyacrylamide using the reactive blending method, there was a stretch of the C=O bond associated with a peak at  $1667\text{ cm}^{-1}$ , and the same vibration for the N–H and C–N bonds was associated with a peak centered on  $1611$  and  $1407\text{ cm}^{-1}$  [24].

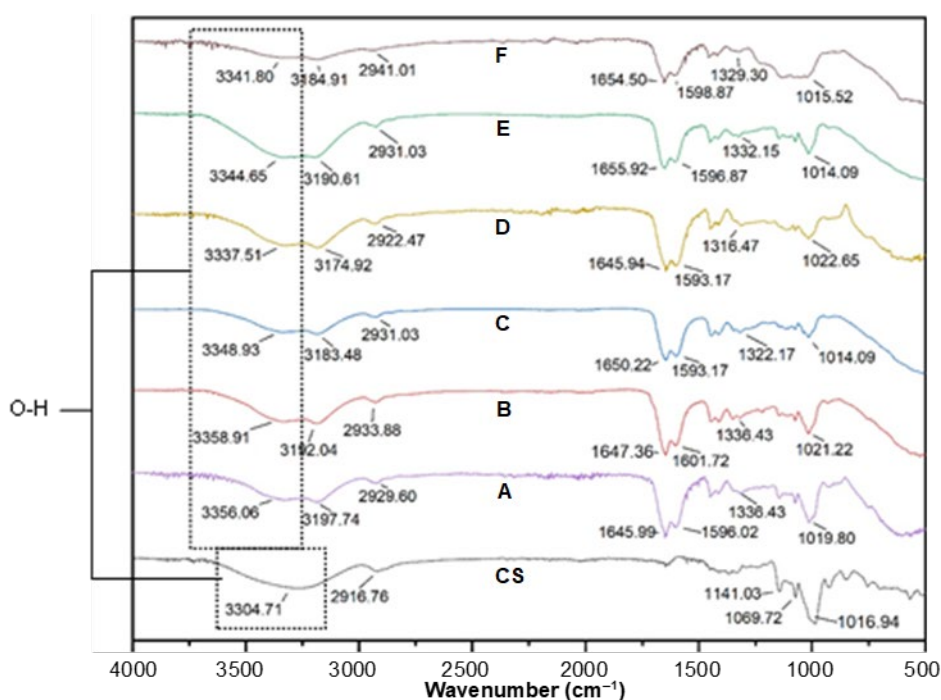


Fig 1. FTIR of CS and CS-g-PAM (A–F)

**Table 2.** Comparison FTIR spectra between CS-g-PAM hydrogel and previous report

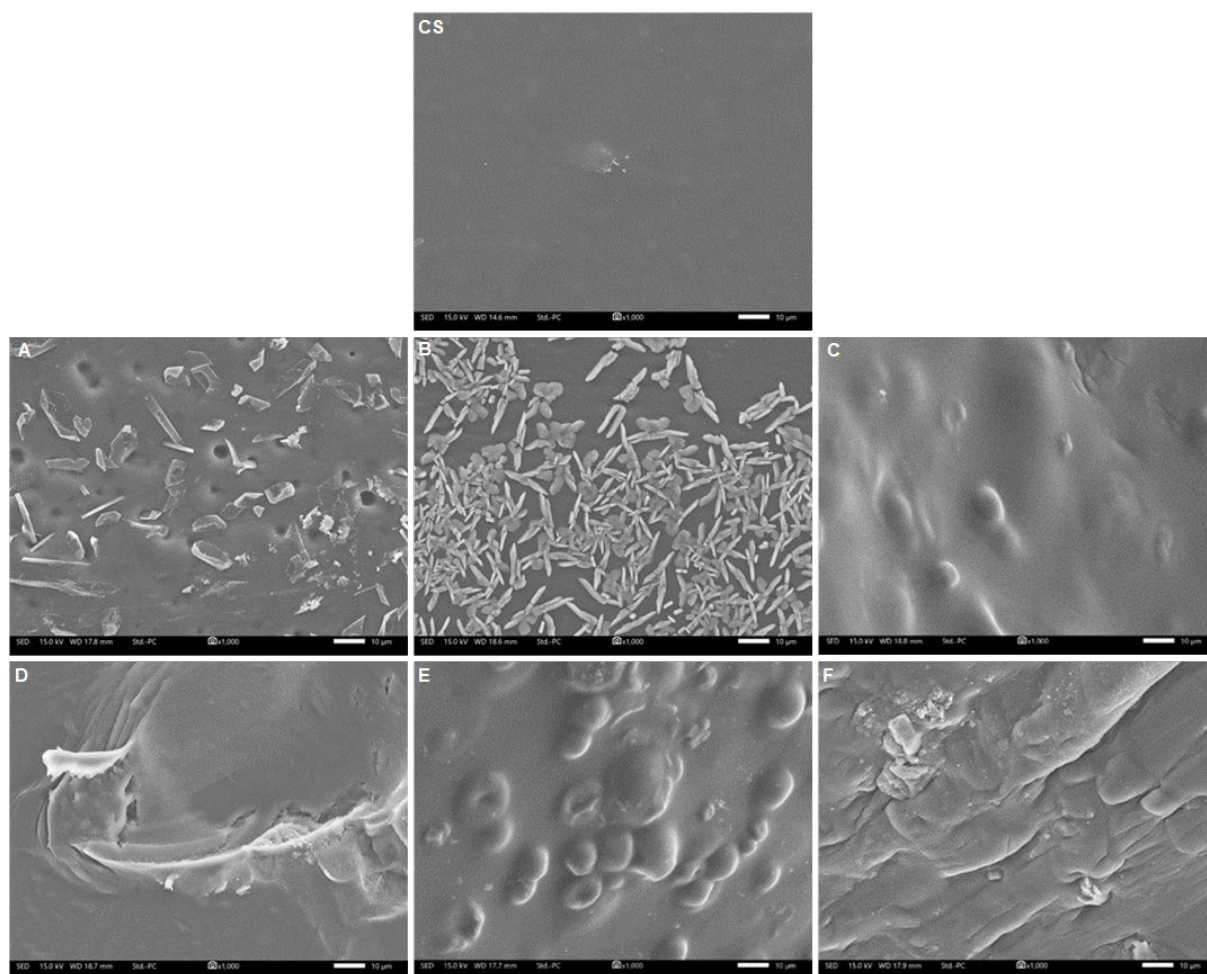
Spectrum	Peak (cm <sup>-1</sup> )		
	CS-g-PAM A	Cassava starch-graft-polyacrylamide [24]	Polyacrylamide grafted xanthan [25]
C=O	1645.99	1667	1675
N-H	1596.02	1611	1615
C-N	1336.43	1407	1410

In the FTIR spectra of the synthesis of polyacrylamide grafted xanthan there was a stretch of the C=O bond associated with a peak at 1675 cm<sup>-1</sup>, and the same vibration for the N-H and C-N bonds was associated with a peak centered on 1615 and 1410 cm<sup>-1</sup> [25]. These peaks appeared in the FTIR spectra of CS-g-PAM (A-F). Thus, the presence of additional peaks in the case of CS-g-PAM (A-F) compared to CS confirmed the success of grafting acrylamide chains in the backbone of CS.

### Scanning Electron Microscope

The microstructure of the surface of CS and CS-g-PAM can be determined by SEM. The SEM photographs of CS and CS-g-PAM are shown in Fig. 2. The SEM of CS-g-PAM shows that it has different surface morphology compared to CS.

The SEM image of CS-g-PAM showed smooth, coarse and rough surfaces. The SEM of CS-g-PAM (B, D, F) with a higher amount of acrylamide, appeared to have a more rough surface. Likewise, with CS-g-PAM (C

**Fig 2.** SEM images of CS and CS-g-PAM hydrogel (A-F)

and D or E and F) with a longer irradiation time. This observation indicated that the higher the amount of acrylamide and the longer irradiation time, the more polyacrylamide chains were grafted onto the backbone of CS.

The SEM of images CS-g-PAM C and E have similar surface morphology, which was caused when the irradiation time stopped and the gel mass was formed. However, E had a rougher surface than C because of the higher amount of acrylamide. The SEM image of CS-g-PAM D and F showed more rough surfaces when the irradiation time was extended to 180 s. The higher the acrylamide amount and the longer the irradiation time caused more polyacrylamide to be grafted onto the backbone of CS, causing more rough surfaces in the morphology results.

The SEM images of CS-g-PAM A and B show that these materials contained granules with shape irregularities, consisting of a number of faces (polyhedral) and relatively sharp edges. Although most of the granules were still separated, some of the granules were connected to each other via the outer layer of the grafted polyacrylamide chain. The irregular structure in the form of connected grains and sharp edges was due to the low acrylamide content. The polyacrylamide grafted onto the backbone of CS was low [26].

The binding of hydroxyl groups, which establish hydrogen and covalent connections between starch chains, causes granules to aggregate, allowing the development of pores suitable for water absorption [27]. CS-g-PAM has a

coarse and broad network and slightly rough surfaces. Coarse, rough and porous surfaces seem to be related to water absorption abilities [24]. The SEM photographs of CS-g-PAM exhibit a coarse and broad network with a rough surface. It was similar to the SEM photograph of chitosan-grafted-polyacrylamides [28] and cassava waste pulp-acrylamide [29]. The morphological differences between CS and CS-g-PAM further supported the successful grafting of polyacrylamide side chains onto the starch backbone.

### Swelling Ratio Measurement

The swelling ratio of CS-g-PAM in distilled water is shown in Fig. 3. The swelling ratio increased from 0 to 120 m of swelling time. The longer irradiation time and the higher amount of acrylamide improved the swelling ratio. The measurement of the swelling ratio aims to determine the potential of hydrogels to decrease reservoir heterogeneity, hence enhancing sweep efficiency during profile improvements in a typical reservoir [30].

The swelling ratio of CS-g-PAM A and B increased from 1.39 to 2.83 g/g as irradiation time increased from 180 to 300 s. The swelling ratio of CS-g-PAM C, D, E, and F increased as the irradiation time for the gel to form was extended to 180 s. These results showed that the swelling ratio of CS-g-PAM is affected by irradiation time.

In the case of CS-g-PAM B, D, and F with an irradiation time of 180 s, the swelling ratio increased from 1.39 to 9.58 g/g as the amount of acrylamide increased from 2 to 10 g. This phenomenon indicated

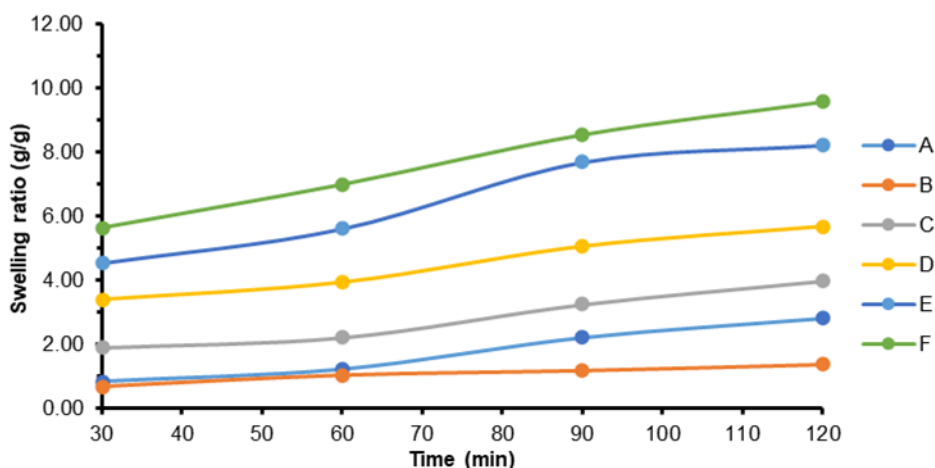


Fig 3. Swelling ratio of CS-g-PAM hydrogel (A-F) in distilled water

that the swelling ratio of CS-g-PAM is influenced by the amount of acrylamide.

The highest swelling ratio was obtained in CS-g-PAM F at 9.58 g/g. The longer irradiation time and the higher amount of acrylamide, the more polyacrylamide will be grafted onto CS. It can be proven in the morphology results that F had the roughest and broadest surface compared to the other products.

Preformed particle gel (PPG) that was synthesized from acrylamide-*N,N*-dimethyl acrylamide-2-acrylamido-2-methylpropane sulfonic sodium salt (AMPSNa)-*N*-vinylpyrrolidone as a plugging agent in reservoirs had a swelling ratio of about 28 g/g in distilled water at room temperature [31]. Hydrogel synthesis from lutensol AT 25 E - methacrylate as chemical enhanced oil recovery (CEOR) had a swelling ratio of 3.1 g/g [32]. From the previous studies of the swelling ratio of CS-g-PAM for EOR applications that have been carried out, it is proven that CS-g-PAM can be applied for EOR.

According to reservoir conditions, the swelling ratio was measured at NaCl concentrations from 0 to 250,000 ppm [31]. The swelling ratio of CS-g-PAM at various concentration of saline water (NaCl) are shown in Fig. 4. The swelling ratio decreased as the NaCl concentration was increased from 0 to 250,000 ppm.

The decrease of the swelling ratio of CS-g-PAM as the NaCl concentration was increased, was indicated by

the interaction between the negatively charged groups and the hydrophilic groups connected to the backbone of CS. When the salt content is increased, the contact between the negatively charged polymer chains with the cationic metal results in incomplete electrostatic interactions, which reduces the osmotic pressure difference between the hydrogel network and the external solution [31-32]. Thus, the swelling ratio of CS-g-PAM decreased at high salinity concentrations.

This well-known phenomenon is frequently observed in ionic hydrogel swelling. The presence of amide groups influences hydrogel swelling (non-ionic). The high charge screening effect and complexing with cations resulted in a decreased swelling capacity in the salt solution [33]. Thus the production of homopolymer decreases the swelling ratio significantly. In the case of CS-g-PAM E and F, the increase in the amount of acrylamide and irradiation time could also promote the production of homopolymers and decrease the swelling ratio more significantly than other CS-g-PAM.

According to reservoir conditions, the swelling ratio was measured at temperatures from 25 to 90 °C in laboratory experiments. The swelling ratio of CS-g-PAM in distilled water at various temperatures is shown in Fig. 5. The swelling ratio of CS-g-PAM decreased from the temperature of 25 to 90 °C. The behavior of decreasing swelling ratio of CS-g-PAM in high temperatures can be

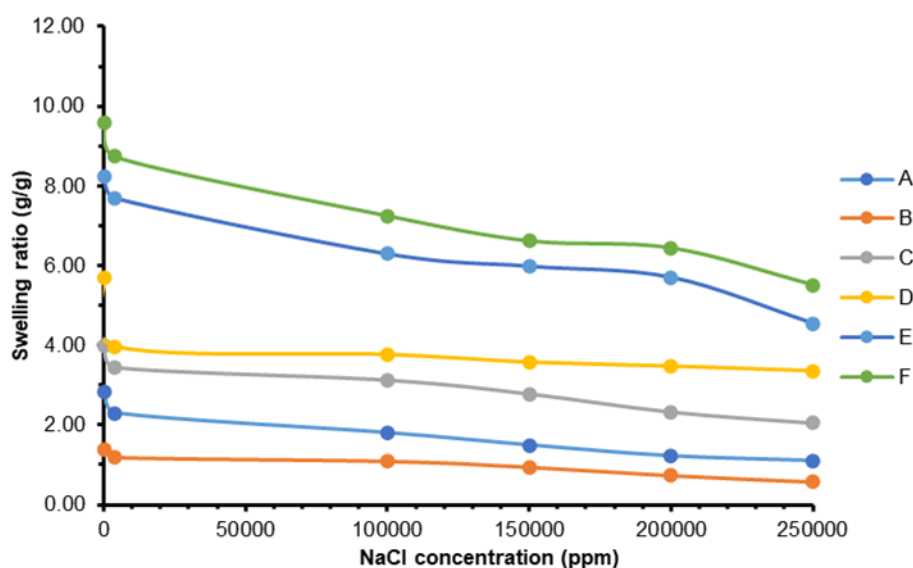


Fig 4. Swelling ratio of CS-g-PAM hydrogel (A-F) at various NaCl concentrations (Swelling time = 120 min)

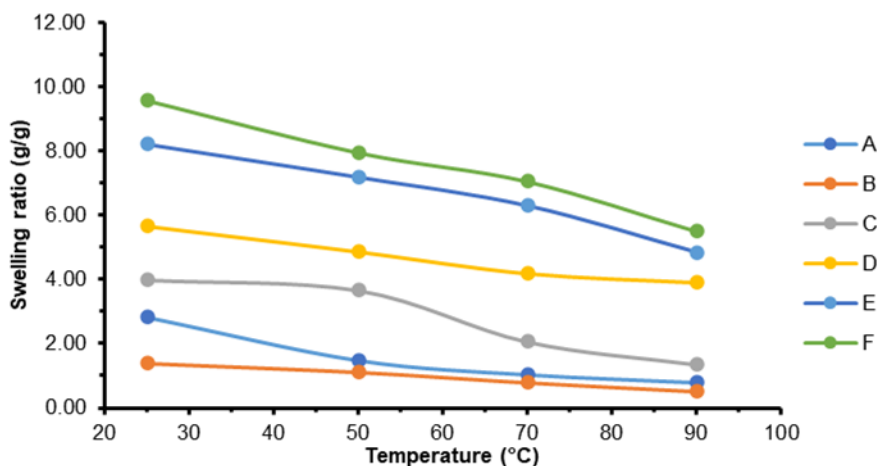


Fig 5. Swelling ratio of CS-g-PAM hydrogel (A-F) at various temperatures (Swelling time = 120 min)

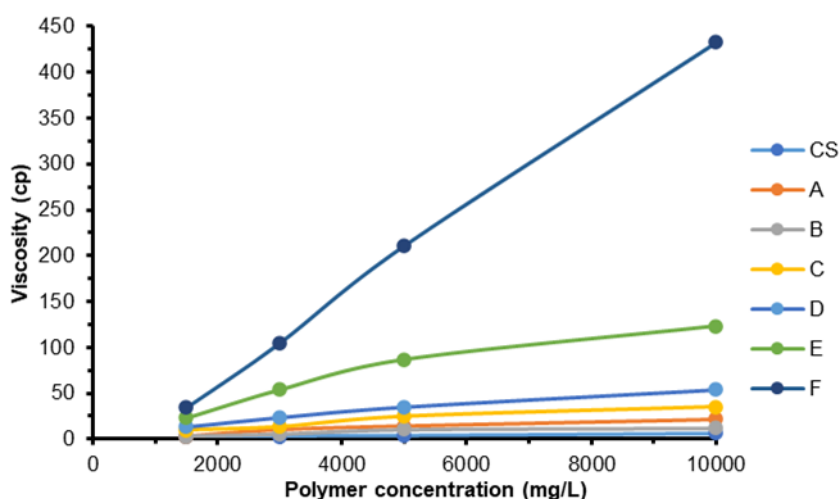


Fig 6. Effect of concentration on CS and CS-g-PAM (A-F) viscosity in distilled water

significantly affected by hydrogen bonding. With increasing temperature, the water molecules trapped in the network are exposed freely when the hydrogen bond interactions become weak or disintegrate and the hydrophobic carbon group interactions become completely dominant [31,34].

In general, the solubility of the polyacrylamide network decreases with increasing temperature and as a consequence the network collapses and the swelling ability is reduced [35]. In the case of CS-g-PAM E and F, the decreasing swelling ratio is significantly caused by the production of homopolymer.

### Water Solubility Measurement

Solubility in the water of CS-g-PAM improved by increasing the amount of acrylamide. Water solubility

increased from 26.72 to 96.06% as the amount of acrylamide increased from 2 to 10 g. The solubility in water also increased with a longer irradiation time. The solubility in water of CS-g-PAM E and F increased from 81.51 to 96.06% with increased irradiation time from 30 to 180 s. Increasing acrylamide concentrations and irradiation time cause improved solubility of the polyacrylamide side chains that lead to a less aggregated and stable grafted starch solution [36].

### Thickening Ability

The viscosity of the polymer solution is an important feature for mobility control. The polymer solution can improve water viscosity and decrease the water-oil mobility ratio, enhancing sweep efficiency [37]. The viscosity of CS and CS-g-PAM that gradually

improved with the concentration of polymer solution are shown in Fig. 6. The polymer in the solution exists as single molecules in the dilution zone, and the viscosity gradually increases. Polymer molecules entangle and even create network structures as polymer concentration increases. The internal frictional motion of the molecules also increased, resulting in increased flow resistance and a significant increase in the viscosity of the polymer solution [16].

The viscosity of the polymer solution increased as the amount of acrylamide and irradiation time increased. The viscosity of CS-g-PAM was several times higher than the viscosity of CS, in the whole polymer concentration range that was investigated. Therefore, grafting polyacrylamide chains onto the CS backbone led to a viscosity increase of the polymer solution. The addition of polyacrylamide increases the viscosity and hence the hydrodynamic volume of CS-g-PAM in water, which may be expressed by destroying the strong intra-hydrogen bonds between the acrylamide units [38].

The viscosity of CS-g-PAM B was slightly higher than the viscosity of CS solution, indicating the small amount of polyacrylamide grafted onto the backbone of CS. This might also indicate that CS-g-PAM B had lower water solubility than the other CS-g-PAM, with water solubility obtained at 26.72%.

The viscosity of the CS-g-PAM solution at various concentrations of NaCl is shown in Fig. 7. For all samples of CS-g-PAM solution, the viscosity decreased with

increasing NaCl concentration. This phenomenon occurred as a result of the addition of a small molecule electrolyte to the system, which modified the polarity of the solution and protected the electrostatic attraction forces within the molecules [16].

CS-g-PAM solution containing polyacrylamide in a low ratio (A, B, C, D) showed a relatively stable viscosity profile compared to NaCl concentration. For CS-g-PAM solution containing polyacrylamide in a high ratio (E, F), a decreasing trend was significant as NaCl concentration was increased. This is due to the "salt out" effect of NaCl on the homopolymer unit of the CS-g-PAM, which causes a shrinkage of the hydrodynamic volume of the polymer and thus lowers the viscosity [38].

A similar observation of the decreased viscosity of polymer solution in saline water is found in the literature, such as the viscosity of the chitosan-AA-AM polymer that decreased from 100 to 20 cp with increasing NaCl concentration from 0 to 40000 mg/L [16]. Starch-g-(PAM-co-PNIPAM) viscosity decreased from 300 to 100 cp with increasing NaCl concentration from 0 to 100,000 ppm [38], which further supports our finding.

The viscosity of CS-g-PAM solution at various temperatures is shown in Fig. 8. The viscosity of CS-g-PAM solution decreased with increasing temperature. Water molecules' thermal mobility increases as the temperature rises and chemical bonds in molecular chains are easily disrupted. Furthermore, the internal rotation of the single bonds in the molecule increased,

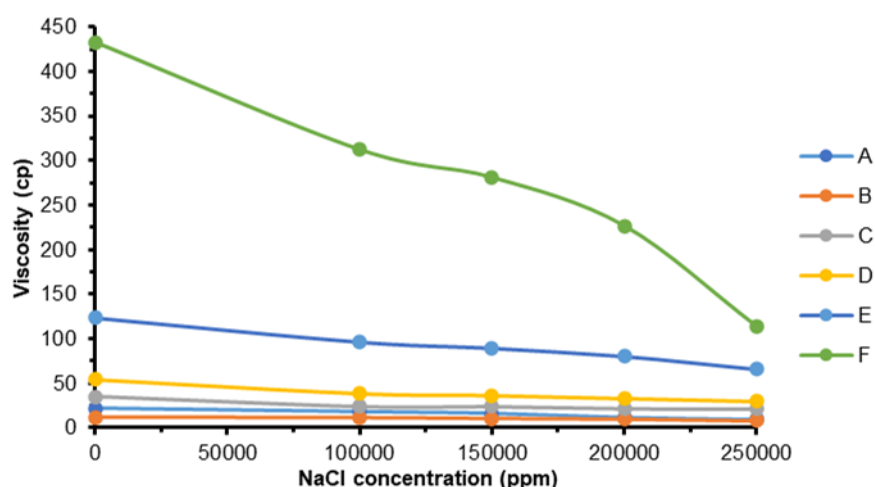


Fig 7. NaCl effects on CS-g-PAM (A-F) viscosity

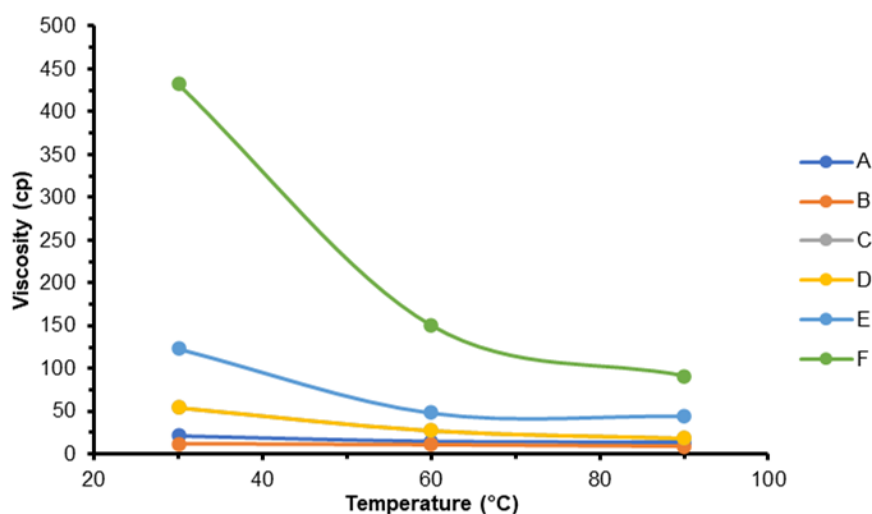


Fig 8. Effect of temperature on CS-g-PAM (A-F) viscosity in distilled water

causing the molecular chain to bend and the associated hydrodynamic radius to decrease [16]. On the other hand, CS-g-PAM solution is susceptible to hydrolysis at high temperatures, which causes a decrease in the viscosity of CS-g-PAM solution. This thermo-responsive behavior is related to breaking strong intra-molecular hydrogen bonds at high temperatures, which is promising for hydrodynamic volume improvement [38].

In the case of CS-g-PAM solution containing polyacrylamide at high ratios (E and F), a decreasing trend was significant as the temperature increased. When the amount of acrylamide and irradiation time in the grafting process are increased, the network between monomers

and CS is strengthened. As a result, the value of grafting percentage increased. However, the increase in the amount of acrylamide and irradiation time could also accelerate the formation of homopolymers and reduce viscosity significantly [39].

A similar observation of the decreased viscosity of polymer solution at various temperatures is found in the literature, such as the viscosity of chitosan-AA-AM polymer that decreased from 350 to 220 cp with increasing temperature from 30 to 90 °C [16]. Starch-g-PAM viscosity decreased from 100 to 60 cp with increasing temperature from 24 to 80 °C [34], further supporting our finding.

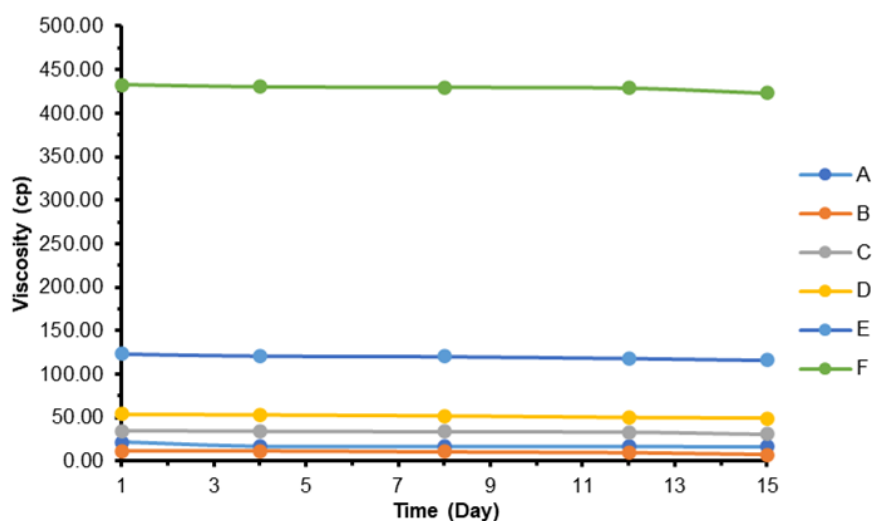


Fig 9. Anti-aging of CS-g-PAM (A-F) solution

### Anti-aging Ability

The viscosity of CS-g-PAM solution in 15 days is shown in Fig. 9. The viscosity of CS-g-PAM solution decreased with increasing aging time. The viscosity of CS-g-PAM solution at 15 days for CS-g-PAM A was 77.66%, CS-g-PAM B was 62.24%, CS-g-PAM C was 88.42%, CS-g-PAM D was 91.24%, CS-g-PAM E was 94.20%, and CS-g-PAM F was 97.85% of CS-g-PAM solution on the first day. This showed that CS-g-PAM F has a good anti-aging ability. The main reason for decreasing the viscosity is that the long molecular polymer chains are broken in the polymer degradation process [40]. As can be seen, with the higher acrylamide amount and longer irradiation time, the viscosity of CS-g-PAM solution was constant with an increasing number of days. Thus, grafting polyacrylamide onto the CS backbone gives a copolymer that has a high and stable viscosity. In other words, grafting polyacrylamide onto starch greatly provides starch resistance to biodegradation [36].

### CONCLUSION

The synthesis of CS-g-PAM by microwave-assisted grafting method and KPS as the initiator has been performed. The FTIR spectra and SEM morphology of CS and CS-g-PAM confirmed the success of polyacrylamide grafted onto the CS backbone by utilizing energy from a domestic microwave.

The results showed that the increasing amount of acrylamide and irradiation time improved the swelling ratio, water-solubility, thickening ability, and anti-aging ability of CS-g-PAM. The data indicated that CS-g-PAM has good thickening, temperature resistance, and salt resistance properties.

CS-g-PAM F prepared with 10 g acrylamide and 180 s of irradiation time exhibited the highest performance compared to the other CS-g-PAM samples. CS-g-PAM F had the highest grafting percentage and water solubility, which was 1565.53 and 96.06%, respectively. CS-g-PAM F had the highest swelling ratio in distilled water which was 9.58 g/g, and still offered the highest swelling ratio at various NaCl concentrations and temperatures. The viscosity of CS-g-PAM F also showed the highest result compared to the other CS-g-PAM samples and exceeded

97% after 15 days of aging, which indicated that CS-g-PAM F has a good performance as a thickening agent and has a good anti-aging ability.

Considering the inexpensive CS, easy synthesis, and resistance of CS-g-PAM to various NaCl concentrations and temperatures according to reservoir conditions, CS-g-PAM can be a good candidate for EOR applications.

### ACKNOWLEDGMENTS

The authors sincerely thank The Directorate General of Higher Education, Indonesia, for financial support of this work through *Penelitian Fundamental* 2021 PNPB Universitas Sebelas Maret with contract number 260/UN27.22/HK.07.00/2021.

### REFERENCES

- [1] Sun, X., Zhang, Y., Chen, G., and Gai, Z., 2017, Application of nanoparticles in enhanced oil recovery: A critical review of recent progress, *Energies*, 10 (3), 345.
- [2] Xu, X., Saeedi, A., and Liu, K., 2017, An experimental study of combined foam/surfactant polymer (SP) flooding for carbone dioxide-enhanced oil recovery (CO<sub>2</sub>-EOR), *J. Pet. Sci. Eng.*, 149, 603–611.
- [3] Wei, B., Romero-Zerón, L., and Rodrigue, D., 2014, Mechanical properties and flow behavior of polymers for enhanced oil recovery, *J. Macromol. Sci., Part B: Phys.*, 53 (4), 625–644.
- [4] Lee, K.S., 2011, Performance of a polymer flood with shear-thinning fluid in heterogeneous layered systems with crossflow, *Energies*, 4 (8), 1112–1128.
- [5] Samanta, A., Ojha, K., Sarkar, A., and Mandal, A., 2013, Mobility control and enhanced oil recovery using partially hydrolyzed polyacrylamide (PHPA), *Int. J. Oil, Gas Coal Technol.*, 6 (3), 245–258.
- [6] Chen, L., Zhu, X., Fu, M., Zhao, H., Li, G., and Zuo, J., 2019, Experimental study of calcium-enhancing terpolymer hydrogel for improved oil recovery in ultradeep carbonate reservoir, *Colloids Surf., A*, 570, 251–259.
- [7] Singh, R., and Mahto, V., 2017, Synthesis, characterization and evaluation of polyacrylamide

- graft starch/clay nanocomposite hydrogel system for enhanced oil recovery, *Pet. Sci.*, 14 (4), 765–779.
- [8] Haruna, M.A., Nourafkan, E., Hu, Z., and Wen, D., 2019, Improved polymer flooding in harsh environments by free-radical polymerization and the use of nanomaterials, *Energy Fuels*, 33 (2), 1637–1648.
- [9] Viken, A.L., Skauge, T., Svendsen, P.E., Time, P.A., and Spildo, K., 2018, Thermo-thickening and salinity tolerant hydrophobically modified polyacrylamides for polymer flooding, *Energy Fuels*, 32 (10), 10421–10427.
- [10] Ghosh, P., and Mohanty, K.K., 2019, Study of surfactant–polymer flooding in high-temperature and high-salinity carbonate rocks, *Energy Fuels*, 33 (5), 4130–4145.
- [11] Pu, W., Shen, C., Wei, B., Yang, Y., and Li, Y., 2018, A comprehensive review of polysaccharide biopolymers for enhanced oil recovery (EOR) from flask to field, *J. Ind. Eng. Chem.*, 61, 1–11.
- [12] Mohd, T.A.T., Manaf, S.F.A., Naim, M.A., Shayuti, M.S.M., and Jaafar, M.Z., 2020, Properties of biodegradable polymer from terrestrial mushroom for potential enhanced oil recovery, *Indones. J. Chem.*, 20 (6), 1382–1391.
- [13] Junlapong, K., Maijan, P., Chaibundit, C., and Chantarak, S., 2020, Effective adsorption of methylene blue by biodegradable superabsorbent cassava starch-based hydrogel, *Int. J. Biol. Macromol.*, 158, 258–264.
- [14] Elsaheed, S.M., Zaki, E.G., Omar, W.A.E., Ashraf Soliman, A., and Attia, A.M., 2021, Guar gum-based hydrogels as potent green polymers for enhanced oil recovery in high-salinity reservoirs, *ACS Omega*, 6 (36), 23421–23431.
- [15] El-hoshoudy, A.N., Hosny, R., Fathy, M., Abdelraheem, O.H., Gomaa, S., and Desouky, S.M., 2019, Enhanced oil recovery using polyacrylates/ACTF crosslinked composite: Preparation, characterization and coreflood investigation, *J. Pet. Sci. Eng.*, 181, 106236.
- [16] Chen, Q., Ye, Z., Tang, L., Wu, T., Jiang, Q., and Lai, N., 2020, Synthesis and solution properties of a novel hyperbranched polymer based on chitosan for enhanced oil recovery, *Polymers*, 12 (9), 2130.
- [17] Nagarpita, M.V., Roy, P., Shruthi, S.B., and Sailaja, R.R.N., 2017, Synthesis and swelling characteristics of chitosan and CMC grafted sodium acrylate-co-acrylamide using modified nanoclay and examining its efficacy for removal of dyes, *Int. J. Biol. Macromol.*, 102, 1226–1240.
- [18] Singh, A.V., Nath, L.K., and Guha, M., 2011, Microwave assisted synthesis and characterization of *Phaseolus aconitifolius* starch-g-acrylamide, *Carbohydr. Polym.*, 86 (2), 872–876.
- [19] Mishra, S., Rani, G.U., and Sen, G., 2012, Microwave initiated synthesis and application of polyacrylic acid grafted carboxymethyl cellulose, *Carbohydr. Polym.*, 87 (3), 2255–2262.
- [20] Mishra, S., Mukul, A., Sen, G., and Jha, U., 2011, Microwave assisted synthesis of polyacrylamide grafted starch (St-g-PAM) and its applicability as flocculant for water treatment, *Int. J. Biol. Macromol.*, 48 (1), 106–111.
- [21] Zhou, P., Ru, X., Yang, W., Dai, Z., Ofori, M.A., Chen, J., Hou, J., Zhong, Z., and Jin, H., 2022, Study on preparation of cationic flocculants by grafting binary monomer on cellulose substrate by  $\gamma$ -ray co-irradiation, *J. Environ. Chem. Eng.*, 10 (2), 107138.
- [22] Kaavessina, M., Fatimah, I., and Soraya, S., 2018, Performance test of starch-g-polyacrylamide synthesized through grafting as a flocculant in artificial wastewater treatment, *EJChE*, 2 (1), 17–23.
- [23] Razali, M.A.A., Ismail, H., and Ariffin, A., 2015, Graft copolymerization of polyDADMAC to cassava starch: Evaluation of process variables via central composite design, *Ind. Crops Prod.*, 65, 535–545.
- [24] Nakason, C., Wohmang, T., Kaesaman, A., and Kiatkamjornwong, S., 2010, Preparation of cassava starch-graft-polyacrylamide superabsorbents and associated composites by reactive blending, *Carbohydr. Polym.*, 81 (2), 48–357.
- [25] Chami, S., Joly, N., Bocchetta, P., Martin, P., and Aliouche, D., 2021, Polyacrylamide grafted xanthan: Microwave-assisted synthesis and

- rheological behavior for polymer flooding, *Polymers*, 13 (9), 1484.
- [26] Lele, V., 2015, Morphological study of graft copolymers of maize starch with acrylamide and methacrylamide, *Int. J. Curr. Res.*, 7 (9), 19991–19994.
- [27] Soto, D., Urdaneta, J., Pernia, K., León, O., Muñoz-Bonilla, A., and Fernández-García, M., 2016, Itaconic acid grafted starch hydrogels as metal remover: Capacity, selectivity and adsorption kinetics, *J. Polym. Environ.*, 24 (4), 343–355.
- [28] Monyake, K.C., and Alagha, L., 2022, Enhanced separation of base metal sulfides in flotation systems using chitosan-grafted-polyacrylamides, *Sep. Purif. Technol.*, 281, 119818.
- [29] Mas'ud, Z.A., Khotib, M., Sari, N., and Nur, A., 2013, Synthesis of cassava waste pulp-acrylamide super absorbent: Effect of initiator and cross-linker concentration, *Indones. J. Chem.*, 13 (1), 66–71.
- [30] El-hoshoudy, A.N., Mohammedy, M.M., Ramzi, M., Desouky, S.M., and Attia, A.M., 2019, Experimental, modeling and simulation investigations of a novel surfmer-co-poly acrylates crosslinked hydrogels for water shut-off and improved oil recovery, *J. Mol. Liq.*, 277, 142–156.
- [31] Farasat, A., Sefti, M.V., Sadeghnejad, S., and Saghafi, H.R., 2017, Effects of reservoir temperature and water salinity on the swelling ratio performance of enhanced preformed particle gels, *Korean J. Chem. Eng.*, 34 (5), 1509–1516.
- [32] Czarnecka, E., and Nowaczyk, J., 2020, Semi-natural superabsorbents based on starch-g-poly(acrylic acid): Modification, synthesis and application, *Polymers*, 12 (8), 1794.
- [33] Sadeghi, M., and Yarahmadi, M., 2011, Swelling and characterization behavior of anti-salt superabsorbent based on carboxymethyl cellulose-g-PAA-co-BuMC hydrogel, *Orient. J. Chem.*, 27 (2), 435–444.
- [34] Abidin, A.Z., Puspasari, T., and Graha, H.P.R., 2014, Utilization of cassava starch in copolymerisation of superabsorbent polymer composite (SAPC), *J. Eng. Technol. Sci.*, 46 (3), 286–298.
- [35] Wedel, B., Hertle, Y., Wrede, O., Bookhold, J., and Hellweg, T., 2016, Smart homopolymer microgels: influence of the monomer structure on the particle properties, *Polymers*, 8 (4), 162.
- [36] Eutamene, M., Benbakhti, A., Khodja, M., and Jada, A., 2009, Preparation and aqueous properties of starch-grafted polyacrylamide copolymers, *Starch/Staerke*, 61 (2), 81–91.
- [37] Chen, Y., He, H., Yu, Q., Liu, H., Chen, L., Ma, X., and Liu, W., 2021, Insights into enhanced oil recovery by polymer-viscosity reducing surfactant combination flooding in conventional heavy oil reservoir, *Geofluids*, 2021, 7110414.
- [38] Fan, Y., Boulif, N., and Picchioni, F., 2018, Thermo-responsive starch-g-(PAM-co-PNIPAM): Controlled synthesis and effect of molecular components on solution rheology, *Polymers*, 10 (1), 92.
- [39] Wang, Z., Shi, H., Wang, F., Wang, A., He, Q., and Cuan, S., 2021, Synthesis of cassava starch-g-acrylic acid/dimethylaminopropyl methacrylamide: A new hydrogel for brine solution, *Carbohydr. Polym.*, 266, 118109.
- [40] Xin, X., Yu, G., Chen, Z., Wu, K., Dong, X., and Zhu, Z., 2018, Effect of polymer degradation on polymer flooding in heterogeneous reservoirs, *Polymers*, 10 (8), 857.